

Fault Location Using Sparse Synchrophasor Measurement of Electromechanical-Wave Oscillations

Ahad Esmaeilian, *Student Member, IEEE*, and M. Kezunovic, *Fellow, IEEE*

Abstract—This paper presents a novel system-wide fault-location method for transmission lines utilizing electromechanical-wave oscillation propagation phenomena. The method uses synchrophasor measurements during disturbances obtained from phasor measurement units sparsely located in the network. The method determines the time of arrival of electromechanical waves propagating from the fault point to sparsely located phasor measurement units. By taking the speed of electromechanical-wave propagation as well as topology of the network into account, the method is able to detect the faulty line. Finally, by adding fictitious buses inside the faulty line and applying a binary search method, the location of fault is accurately pinpointed. The main advantage of the proposed method is the use of a limited number of PMUs which reduces the cost of implementation. The method was developed in MATLAB and tested with the IEEE 118-test system. Test results reveal the high accuracy of the method in detecting and locating faults.

Index Terms—Electromechanical-wave propagation, fault detection, fault location, phasor measurement units (PMUs), power system faults, synchrophasor measurement, wide-area measurements.

I. INTRODUCTION

POWER system is subjected to faults caused by various reasons such as different weather condition, animal or human contacts, vegetation contacts, etc. Once circuit breakers clear the fault following relays trip command, the fault point must be determined and proper action taken to expedite troubleshooting and minimize repair time [1].

Various fault location methods have been proposed in literature [2]–[23]. Single-end impedance based fault location methods are considered the most conventional scheme [2]–[8]. These methods utilize power frequency component of single-end voltage and (or) current measurements to locate faults on transmission lines. The main advantage of such methods is the simplicity and low cost of implementation. However, their accuracy might be affected by different factors, such as infeed current from remote end, fault resistance, varia-

tion of source impedance, loading conditions or fault incidence angle.

Several methods were developed using unsynchronized two-end measurements [9]–[13]. In [9], post fault voltage and current phasor measurements are used to locate faults. The method is applicable even if line parameters are unknown. In [10], symmetrical components theory is used to formulate fault location scheme. The method proposed in [11] is based on voltage magnitude at fault point and does not require phase angles. In [14], a time-domain method based on synchronized sampling of the voltage and current data from the two ends of the line is proposed. The line model equations are then solved to build the voltage and current profiles to accurately locate the fault. Improving the line model considering distributed line parameters led to more accurate results in [15]. In [16], the method proposed in [15] was modified to reduce the sampling rate from 20 kHz to 1 kHz. The main advantage of the mentioned two-end fault location methods comparing to single-end methods is their higher accuracy in locating faults. However, availability of measurements through the entire network might not be feasible due to the cost and installation concerns for foreseeable future [1]. Hence, a sparse measurements based fault location method could be more practical due to its low implementation cost.

In recent decades, development of phasor measurement units (PMUs) introduced various synchrophasor based methods [17]–[20]. In [17], [18], Clarke transformation is applied to the synchronized voltage and current phasors aligned with a discrete Fourier transform-based algorithm to calculate the location of fault. Another fault detection/location technique is presented in [19], [20] with consideration of arcing fault discrimination based on synchronized fundamental phasor measurements. In [21], a bus-impedance matrix was utilized to calculate fault point with access to limited synchronized measurements at two remote buses in the network.

Several methods utilize electromagnetic transient propagation in power system and are known as travelling wave based methods [22]–[25]. The method proposed in [22], [23] is based on measuring time of arrival (ToA) of electromagnetic traveling waves which propagate from the fault point to sparsely located synchronized measurement devices. Then, an optimization method is applied to calculate the location of fault. In [24], a wide area traveling wave based method is proposed which determines faulty line and distance to fault by analyzing the traveling wave propagation times using the extended double end

Manuscript received June 30, 2015; revised September 26, 2015 and November 30, 2015; accepted December 15, 2015. Date of publication December 29, 2015; date of current version July 21, 2016. Paper no. TPWRD-00831-2015.

The authors are with the Department of Electrical and Computer Engineering, Texas A&M University, College Station, TX 77843-3128 USA (e-mail: ahadesmaeilian@tamu.edu; kezunov@ece.tamu.edu).

Color versions of one or more of the figures in this paper are available online at <http://ieeexplore.ieee.org>.

Digital Object Identifier 10.1109/TPWRD.2015.2510585

method. In [25], a traveling wave principle along with two graph theory-based lemmas is deployed to sectionalize power system and locate faults within suspected sections. Despite the high accuracy of travelling wave based methods, they require measurement device with high sampling rate to capture electromagnetic transient which increase cost of implementation.

The method proposed in this paper is based on detection of ToA of electromechanical-wave oscillation propagates in power system. Despite electromagnetic traveling wave based methods, the proposed method relies on sparse PMU measurements, and can be practically used by utilities without requiring expensive dedicated high sampling rate devices. Section 2 gives the background theory while Section 3 explains the methodology. The results from testing are given in Sections 4 and 5 gives conclusions.

II. BACKGROUND THEORY

A. Electromechanical-Wave Propagation Phenomena

When a disturbance occurs on a transmission line, electrical power flow changes in the network. This leads to a mismatch between electrical and mechanical torque of generators located in the vicinity. Therefore, each generator rotor angle changes to compensate the mismatch. Following the generators' rotor angle oscillations, the adjacent buses also encounter changes in their generators' rotor angle which again causes a mismatch in the electrical torque of the adjacent generators. In this fashion, the oscillation known as the electromechanical-wave propagation is "seen" throughout the entire network. Electromechanical oscillations could be detected by monitoring phasor angle of bus voltages and characterized with much lower frequency (0.1–10.0 Hz) than electromagnetic transients (>100 kHz) [26]. To illustrate the concept, a simple power-system model in the form of a ring is used. Fig. 1(a) shows the 64-generator ring system introduced in [26], which comprises 64 identical serially connected generators through identical transmission lines, forming a ring. The initial bus angles are evenly distributed from 0 to 360 degrees by steps equal to $360/64 = 5.625$ degrees. Due to homogeneity and ring shape of the 64-bus system, it is well-suited to study basic aspects of electromechanical-wave propagation phenomena. Fig. 1(b) shows the phasor angle of 64-buses (in radian) with respect to time of a given disturbance occurring at bus 16 at $t = 0$. Following the change in the angle of bus 16th shown by the dashed line in Fig. 1(b), the other generators react in a similar fashion, but with a certain time delay. Plotting all the bus angles together, this time delay can be represented as a wave modulated on buses' phasor angles, which travels away from the disturbance source into the network at a finite speed.

B. Continuum Modeling

Applying differential algebraic equations (DAEs) is the conventional way of modeling electromechanical-wave propagation in power system. Due to complexity, this approach could be time consuming and the result would be hard to analyze for large networks. Therefore, researchers introduced a much

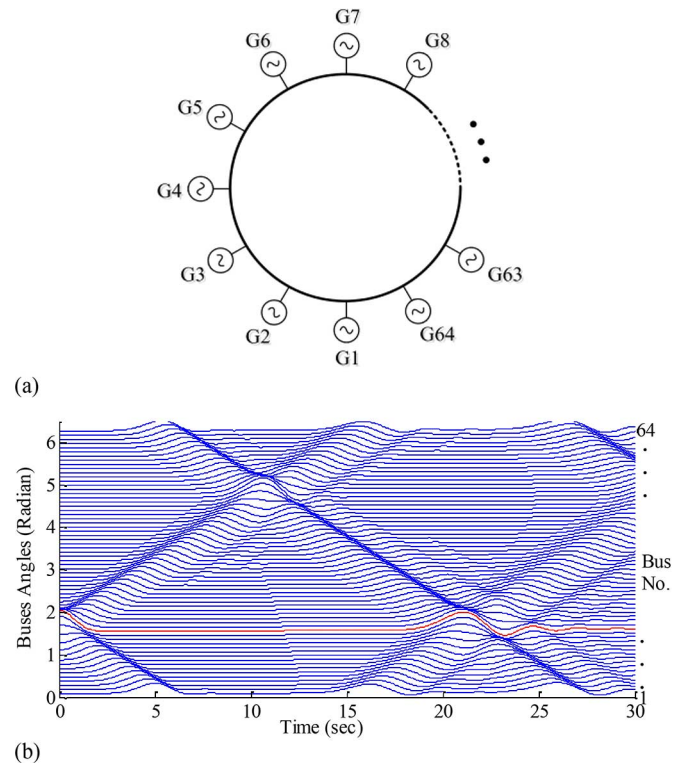


Fig. 1. Understanding electromechanical-wave propagation. (a) 64-generator ring system, (b) Bus angle modulation following a fault at bus 16 at $t = 0$.

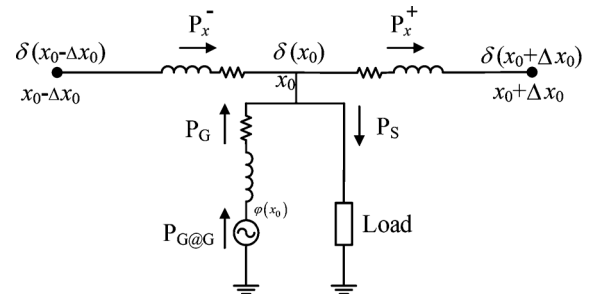


Fig. 2. Incremental system used for continuum modeling of system at x_0 .

simpler method which embeds the effect of electromechanical-wave propagation into power system behavior [26]–[30].

The so called continuum model, considers power system with spatially distributed parameters. The continuum model is based on applying partial differential equations (PDEs) describing the power systems to the infinitesimal element distributed along the power system. Due to generators rotor inertia, the timescale of electromechanical oscillations is large compared to the power system frequency. Therefore, the variables in continuum model can be considered as phasor parameters [30].

In the context of continuum modeling, any point in power system could be represented by the incremental system as shown in Fig. 2. The model allows for representation of lines with different per-unit impedances, shunt reactances, generators and loads. The flexibility of the incremental model allows any arbitrary network topology to be modeled with continuum approach. Following is a brief summary of continuum formulation.

In Fig. 2, the net real electrical power flow at point x_0 can be written as (1), shown at the bottom of the page, where $\delta(x)$ represents the phase angle of voltage at x . R , X and Z represent resistance, reactance and impedance of the branch, respectively. Using Taylor series expansion about x_0 , and disregarding higher order terms we get:

$$P = \frac{R}{|Z|^2} \left(\frac{\partial \delta(x_0)}{\partial x} \right)^2 \Delta x - \frac{X}{|Z|^2} \frac{\partial^2 \delta(x_0)}{\partial x^2} \Delta x \quad (2)$$

The real power produced at the generator terminal is determined by (3), shown at the bottom of the page. The real power delivered to the point x_0 by the generator is given by (4), shown at the bottom of the page, where G_{int} and B_{int} represent conductance and susceptance of a generator. By conservation of power, the summation of power at a region must be zero, which implies:

$$P = P_G - P_s \quad (5)$$

where P is the net real power flow at x_0 , P_G is real power delivered by generator and P_s is the real power consumed by the load. Plugging (2), (3) and (4), shown at the bottom of the page, into (5), we obtain:

$$G \left(\frac{\partial \delta(x_0)}{\partial x} \right)^2 - B \frac{\partial^2 \delta(x_0)}{\partial x^2} = G_{int} [\cos(\delta(x_0) - \varphi(x_0)) - 1] - B_{int} \sin(\delta(x_0) - \varphi(x_0)) - G_S \quad (6)$$

which is known as continuum equivalent of load flow equations of the power system.

On the other hand, the internal generator phase angle dynamics are modeled using:

$$m(x_0) \frac{\partial^2 \varphi(x_0, t)}{\partial t^2} + d(x_0) \frac{\partial \varphi(x_0, t)}{\partial t} = P_m(x_0) - \frac{P_{G@G}(x_0)}{\Delta x} \quad (7)$$

where $m(x_0)$ and $d(x_0)$ are the generator inertia and damping constant and $P_m(x_0)$ is the mechanical power of a generator. Plugging (3) into (7), we obtain (8), shown at the bottom of the

page, which is known as continuum equivalent of swing equations of the power system. The simulation studies of this paper were carried out using continuum PDE equations (6) and (8).

III. FAULT LOCATION METHODOLOGY

As mentioned earlier, electromechanical wave originated following a disturbance travels with finite velocity in a given network. Since these waves propagate through different paths, they reach remote buses with distinct time delays which depend on each path length and propagation speed of wave through that path. Therefore, one can determine the fault location by using ToA measurements at various locations along with supporting information to determine each path's length and speed of propagation through that path.

The method proposed in this paper detects ToA of electromechanical waves modulated on phasor angle of voltage at selected buses where PMUs are available. Then the well-known Dijkstra's shortest path algorithm [31] is deployed combined with several mathematical steps to detect the faulty line. Finally location of the fault will be determined inside faulty line using binary search method. Fig. 3 shows the implementation structure of the proposed method. Phasor measurements at certain substations throughout entire network can be captured by PMUs or any other IED devices located in that substation, which can measure and report GPS synchronized phasors. The measurements are then transferred to the control center where phasor data concentrator receives data from all PMUs and stores them in real-time database. The database provides input data to the proposed method. The details of the methodology are explained next.

A. ToA and Fault Type Detection

The proposed Artificial Neural Network (ANN) method detects ToA of electromechanical wave modulated on phase angle of voltage based on analyzing the first swing of the phase angle at buses where PMUs are installed. One time calculation utilizing numerous training data sets on ANN implemented using MATLAB ANN toolbox led to an accurate ToA detector.

$$P = \frac{R}{\Delta x |Z|^2} [1 - \cos(\delta(x_0) - \delta(x_0 \pm \Delta x))] + \frac{X}{\Delta x |Z|^2} [\sin(\delta(x_0) - \delta(x_0 \pm \Delta x))] \quad (1)$$

$$P_{G@G}(x_0) = \Delta x G_{int} [1 - \cos(\delta(x_0) - \varphi(x_0))] - \Delta x B_{int} \sin(\delta(x_0) - \varphi(x_0)) \quad (3)$$

$$P_G(x_0) = \Delta x G_{int} [\cos(\delta(x_0) - \varphi(x_0)) - 1] - \Delta x B_{int} \sin(\delta(x_0) - \varphi(x_0)) \quad (4)$$

$$m(x_0) \frac{\partial^2 \varphi(x_0, t)}{\partial t^2} + d(x_0) \frac{\partial \varphi(x_0, t)}{\partial t} = P_m(x_0) + B_{int} \sin(\delta(x_0) - \varphi(x_0)) - G_{int} [1 - \cos(\delta(x_0) - \varphi(x_0))] \quad (8)$$

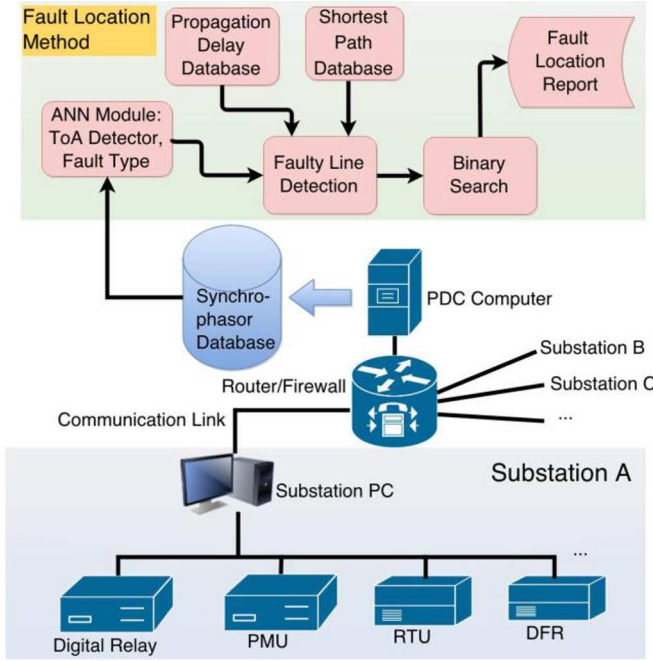


Fig. 3. Fault location method implementation overview.

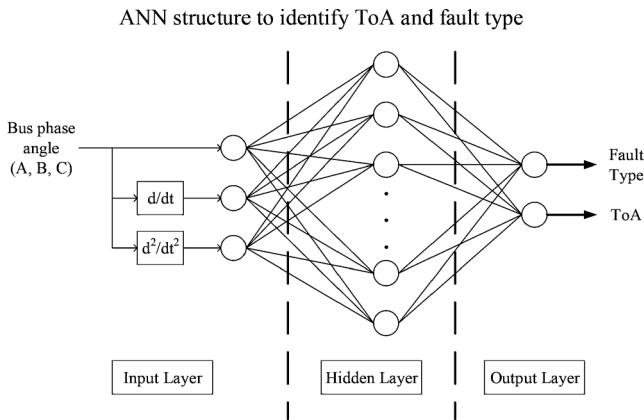


Fig. 4. The network structure of the back propagation neural network model used in ToA detector.

To develop the ToA detector, supervised training is used to train the ANN. Fig. 4 shows the overall structure of deployed ANN. To differentiate between faults and other disturbances as well as different types of fault, three types of input signals were defined in the input layer. The phase angles of each three phase voltages, as well as their first and second time derivatives were selected as inputs. The inputs and desired outputs were compared in a hidden layer and errors are then propagated back through the system. We calculated the performance of the system in terms of number of neurons in the hidden layer, and selected 4 hidden neurons as it provides the best result. The back propagation algorithm causes the ANN system to tweak weights which control the neural network [32]. This process occurs continually till the weights are adjusted within a defined threshold. The applied multilayer perceptron neural network with back propagation algorithm used in this study is one of most common ANN method applied in power system. The desired output of the

ANN is the event type and ToA of the electromechanical wave modulated on voltage phase angle.

In the ANN training process, a set of 2000 events were created within IEEE 118 bus test system [33]. In the training process, all lines are considered to be in service. Training scenarios include generator and load outages, various types of faults with different fault resistance at different locations. Then, another set of 500 previously unseen randomly generated event scenarios (ratio of unseen test cases to trained cases is equal to 0.25) were created to test and validate ANN-based ToA and fault type detector. Since the nature of electromechanical-wave oscillation propagation and its related phase angle modulation is same for different networks, the ANN based ToA detector can be used for any given network.

B. Detection of Faulty Line

Once the ToA of electromechanical-wave oscillation is obtained at selected buses where PMUs are installed, it can be used to determine the faulty line. Several mathematic steps as described below must be deployed before the faulty line could be detected.

1) *Computation of Line Propagation Delay*: As previously stated in Section II, the speed of electromechanical-wave propagation is quite lower compared to electromagnetic one, which is close to speed of light. The researchers proved that applying continuum approach, the speed of electromechanical-wave propagation through the network solely depends on system parameters and can be obtained as follows [26].

$$v = \sqrt{\frac{\omega \sin \theta}{2h|z|}} \quad (9)$$

where ω is the nominal system frequency, θ is the line impedance angle ($\sim 90^\circ$), h is the inertia constant of generator and $|z|$ is the line impedance.

Therefore, the propagation delay of each line in the network can be calculated by:

$$T_{delay-L} = \frac{x_L}{\sqrt{\frac{\omega \sin \theta}{2h|z|}}} \quad (10)$$

where $L = 1, \dots, l$ represents each transmission line in the network and x_L is the total length of line L. Assuming that length and impedance of transmission lines are known, electromechanical-wave propagation delay through each transmission line can be calculated using (10).

2) *Calculation of Measured ToA Matrix*: Fig. 5 is used to explain computation of the shortest time delay matrix. As shown in Fig. 5, for the given network assume that PMU measurements are available at buses A, B, C and D, while a fault occurs at an unknown bus k (this assumption will be removed later). The propagation delay of electromechanical wave to reach bus A after fault occurs at bus k can be obtained by:

$$t_{Ak} = t_A - t_k \quad (11)$$

where t_k represents fault initiation time at bus k , t_A represents ToA of electromechanical wave at bus A and t_{Ak} is the propagation delay of electromechanical wave to arrive at bus A. Since the fault initiation time t_k is unknown, it is impossible to obtain

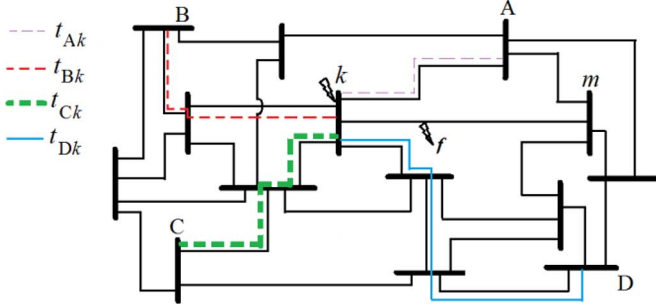


Fig. 5. Illustration of the calculation of theoretical and measured delay matrices.

t_{Ak} . Suppose that bus A is the first to receive the propagated wave. It can be used as the time reference. Therefore, the wave propagation delay from bus k to bus B with respect to ToA of electromechanical wave at bus A (t_A) can be defined as:

$$t_{BA} = t_{Bk} - t_{Ak} = (t_B - t_k) - (t_A - t_k) = t_B - t_A \quad (12)$$

It should be noted that (12) is always correct due to the fact that the electromechanical waves propagate along the transmission lines always following the shortest path rule.

The electromechanical-wave propagation delay from bus k to other buses with respect to ToA of electromechanical wave at bus A (t_A) can be defined similar to (12). Hence, the measured propagation time delay matrix can be defined as:

$$T_{meas} = [t_{BA} \quad t_{CA} \quad t_{DA}] \quad (13)$$

3) *Calculation of Theoretical Time Delay Matrix*: Since the propagation delay of each transmission line is known by (10), vector of time differences resulting from the shortest propagation delay could be computed as follows.

$$T_{sp-x} = [\tau_{Bx} - \tau_{Ax} \quad \tau_{Cx} - \tau_{Ax} \quad \tau_{Dx} - \tau_{Ax}] \quad (14)$$

where τ_{Ax} , τ_{Bx} , τ_{Cx} and τ_{Dx} are the theoretical shortest propagation time delay from buses A, B, C and D to any arbitrary bus x , respectively. It can be rewritten as:

$$T_{sp-x} = [\tau_{BAx} \quad \tau_{CAx} \quad \tau_{DAx}] \quad (15)$$

The shortest time delay path for each bus pair is computed utilizing the Dijkstra's algorithm. One time computation of (15) with Dijkstra's algorithm is valid for a given topology before any line switching takes place. After any topology changes, the calculation must be repeated to update the matrix elements.

4) *Definition of Minimum Error Function*: As shown in Fig. 5, if the fault occurs at unknown bus k , the calculated T_{sp-k} should identically match T_{meas} captured by ToA detectors. Therefore, one can define P_x as follows and then check it for all buses to find the bus that corresponds to the minimum (zero) P_x value.

$$P_x = \text{Min}(\|T_{sp-x} - T_{meas}\|) \quad x = 1, \dots, n \quad (16)$$

where $x = 1, \dots, n$ is the total number of buses and P_x is the minimum norm linked with bus x .

As stated before, we assumed that faults only take place at buses, which is not realistic in actual power system. Conse-

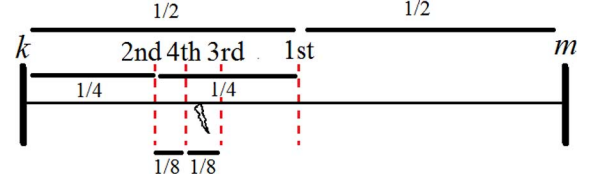


Fig. 6. Illustration of the binary search used for fault location method.

quently, the methodology must be revised, so that the method can be applied for any arbitrary fault located along transmission lines.

As shown in Fig. 5, if the fault occurs at an arbitrary point f , two buses corresponding to the minimum two values obtained from (16) will be selected. The network topology will be checked to see if this pair of buses has a direct link to each other. If so, the line connecting these two buses will be declared as faulty line.

If there is no direct link between the two buses, then each line connected to the two buses will be considered as the faulty line candidate. Hence, fault location calculation must be repeated for all possible candidates which can be tolerated due to limited number of lines connected to the pair of suspect buses.

C. Fault Location Using Binary Search

Once the faulty line is determined, the exact location of fault can be derived by adding fictitious buses and dividing the faulty line into two line segments (binary search approach [32]). As shown in Fig. 6, the first fictitious bus divides the faulty line ($m-k$) into two equal sections (a_1-m and a_1-k). Then, (16) will be recalculated for $x = a_1, m$ and k . Then, the two buses which correspond to lowest P_x values will be treated as faulty section. Similarly, the second fictitious bus divides the faulty section (a_1-k in Fig. 6) into equal sections (a_1-k and a_2-k) and so on. If this process occurs over and over, mathematically, after adding i^{th} fictitious bus, the location of fault will be determined within the following error:

$$E = \left(\frac{1}{2^i}\right) \times 100 \quad (17)$$

In this study, we considered adding 5 fictitious buses to reach accuracy greater than 99%.

IV. TEST RESULTS

In this section, the proposed method is tested using IEEE118 bus test system [35]. The simulation is done by developing MATLAB script based on solving PDE equations obtained from continuum approach. The proposed methodology does not require optimal PMU placement. To avoid an arbitrary placement of PMUs, suggested optimal PMU placement studied in [36] is used to demonstrate the effectiveness of the proposed method for a given PMU optimal placement driven by other applications.

A. Testing With Different Fault Scenarios

In this subsection, the proposed method is tested by changing fault parameters (fault resistance, fault distance, fault type and faulty line). Table I brings summary of results for a few test

TABLE I
FAULT LOCATION RESULTS UNDER DIFFERENT FAULT SPECIFICATION

Case no.	Faulty line	Fault type	Fault resistance (Ω)	Fault distance (p.u.)	Fault location error (%)
1	19-20	a-g	1	0.1	0.73
2				0.5	0.59
3				0.9	0.34
4			20	0.1	1.23
5				0.5	0.92
6				0.9	0.74
7		ab-g	1	0.1	0.56
8				0.5	0.51
9				0.9	0.49
10			20	0.1	0.84
11				0.5	0.83
12				0.9	0.77
13	100-106	ab	1	0.1	0.44
14				0.5	0.47
15				0.9	0.62
16			20	0.1	0.75
17				0.5	0.67
18				0.9	0.93
19		abc-g	1	0.1	0.17
20				0.5	0.14
21				0.9	0.15
22			20	0.1	1.11
23				0.5	0.96
24				0.9	1.04

cases. In all cases, the proposed method correctly detects fault type using proposed ANN module and then identifies faulty lines. Furthermore, the associated fault location error for each case demonstrates that the proposed method is able to accurately locate faults (in most cases error is within 1%).

Fig. 7 represents the phasor angle captured by PMUs related to cases 6, 13 and 20 from Table I (only 4 phasor angles from PMUs with smallest ToAs were plotted to avoid confusion). In Fig. 7(a), the electromechanical-wave oscillation following the fault (a-g with 20Ω at 0.9 pu from bus 19) on line 19-20 is first detected at bus 21 at $t = 5.43$ sec and then detected at buses 15, 23 and 17, respectively. In Fig. 7(b), the electromechanical wave following the fault (ab with 1Ω at 0.1 pu from bus 19) on line 19-20 is first detected at bus 21 at $t = 5.97$ sec and then detected at buses 15, 17 and 30, respectively. In Fig. 7(c), the electromechanical wave following the fault (abc-g with 1Ω at 0.5 pu from bus 100) on line 100-106 is first detected at bus 94 at $t = 5.66$ sec and then detected at buses 105, 110 and 80, respectively. In each case, after detection of ToAs of electromechanical-wave oscillations at PMU locations, T_{meas} and P_k will be calculated from (13) and (16), respectively. The location of faults for these three examples are calculated using proposed binary search method with error equal to 0.74%, 0.44% and 0.14%, respectively.

Table II shows the average error percentage of the proposed fault location method under numerous test cases. As depicted in Fig. 8, IEEE 118 bus system can be divided into three areas with almost same number of PMUs. We considered 9 points to insert faults (0.1 pu to 0.9 pu with span of 0.1 pu) on every single line in these three areas. It can be concluded from results in Table II that area 1 which has higher ratio of PMU to line (0.216) is

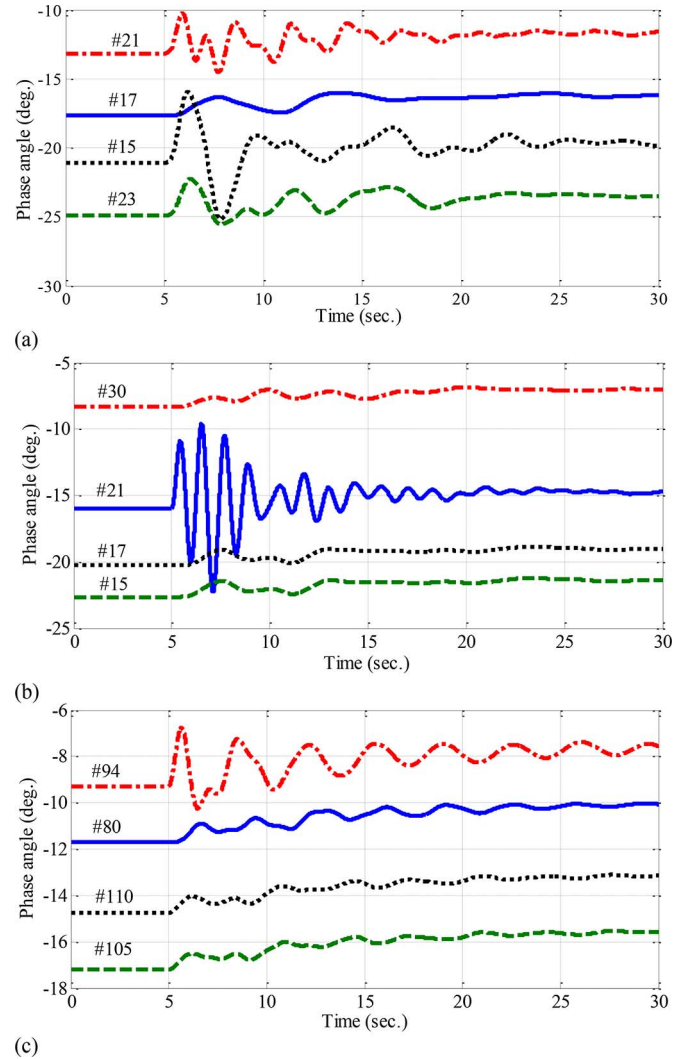


Fig. 7. Phasor angle of PMU equipped buses of IEEE118 bus system, (a) case 6, (b) case 13, (c) case 20.

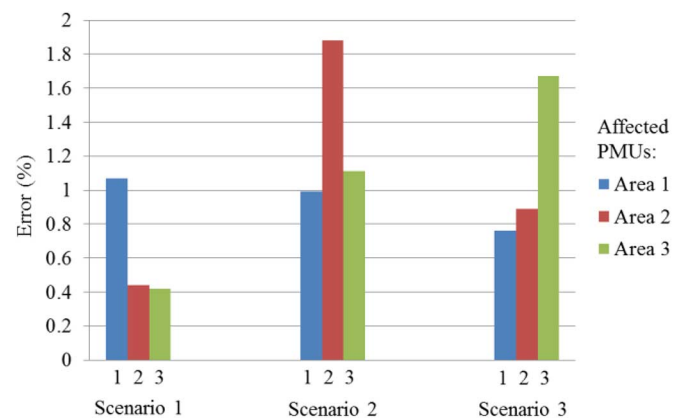


Fig. 8. Fault location error under effect of PMU bad data.

linked with least average error. However, area 2 which has lower ratio of PMU to line (0.147) has the highest average error.

B. Impact of PMU Bad Data

One of the main concerns for applications based on wide area measurements is the accuracy and calibration of PMUs. Since,

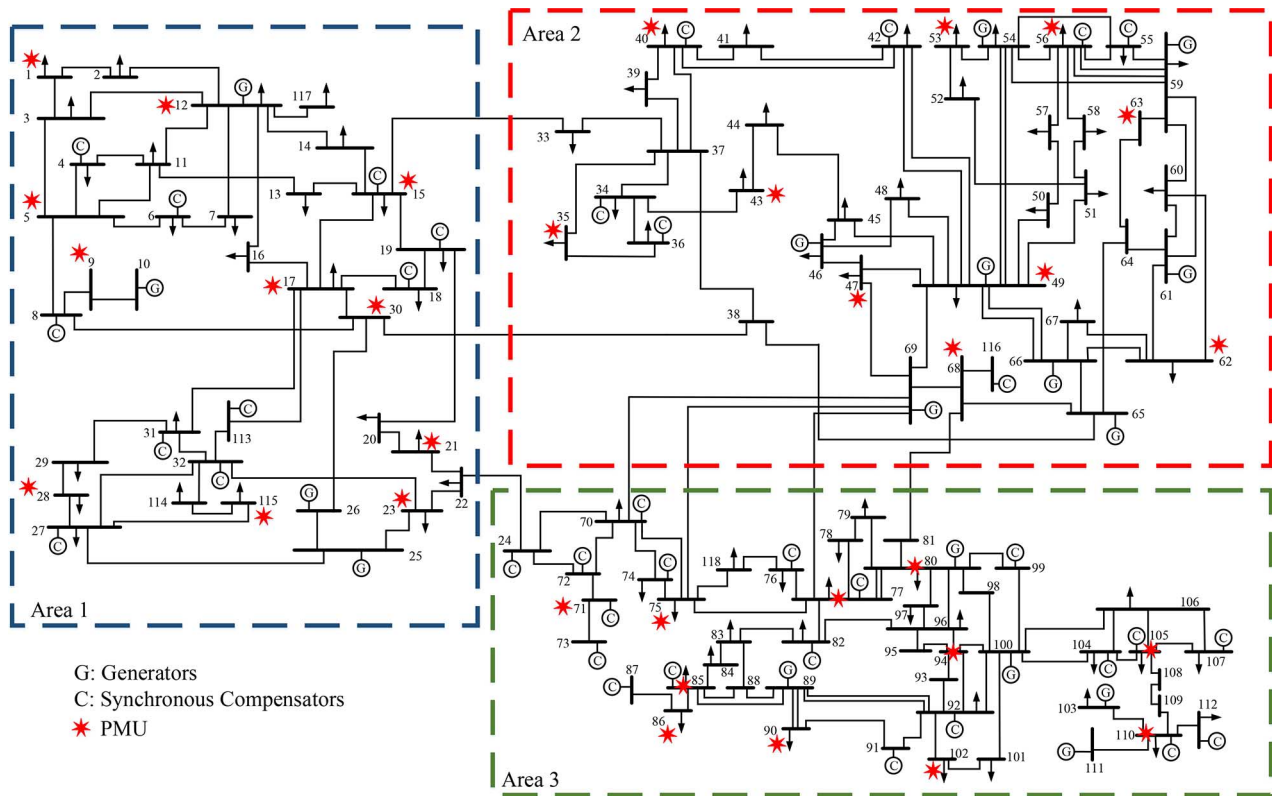


Fig. 9. IEEE 118 bus test system.

TABLE II
FAULT LOCATION RESULTS ON DIFFERENT REGIONS

Area	Number of lines	Number of PMUs	PMU/Line ratio	Fault location error (%)
Area 1	51	11	0.216	0.352
Area 2	68	10	0.147	0.978
Area 3	67	11	0.164	0.754
Total	186	32	0.172	0.724

PMU measurements might be affected due to inaccuracy of algorithms for certain input frequencies or being out of calibration. To test the methodology against such conditions, different test cases were simulated by artificially adding error to phasor angle measurements.

Fig. 8 shows the average error percentage of proposed fault location method under three main scenarios. In scenario 1, the first column represents the average error percentage corresponding to 20 fault cases simulated to occur in area 1 (see Fig. 9), while the manipulated PMU measurements are among PMUs within area 1. Similarly, the second and third columns show the average errors corresponding to same faults in area 1, while the manipulated PMU measurements are among PMUs within area 2 and 3, respectively. It can be seen that the effect of PMU bad data is felt when the affected PMUs are in the same area as the faults are located. The same can be concluded from the second and third scenarios where faults occurred in area 2 and area 3, respectively. Finally, from the results one can conclude that PMU bad data will affect the accuracy of the proposed fault location. However, the methodology is still able to operate within an acceptable error (less than 2%).

TABLE III
IMPACT OF TOPOLOGY CHANGES ON FAULT LOCATION

Case no.	Faulty line	Switched off line	Error before topology change (%)	Error after topology change (%)
Switched line does not contribute in shortest path				
1	1-2	55-59	0.32	0.32
2	25-27	34-37	0.44	0.44
3	41-42	78-79	0.86	0.86
4	76-118	37-39	0.49	0.49
5	110-112	12-117	0.97	0.97
Switched line contributes in shortest path but located far from fault point				
6	1-2	20-21	0.32	0.47
7	25-27	63-64	0.44	0.61
8	41-42	15-17	0.86	0.89
9	76-118	47-69	0.49	0.93
10	110-112	68-81	0.97	0.99
Switched line contributes in shortest path and located close to fault point				
11	1-2	3-5	0.32	-
12	25-27	27-28	0.44	5.98
13	41-42	40-41	0.86	7.41
14	76-118	77-82	0.49	4.75
15	110-112	94-100	0.97	3.64

C. Impact of Topology Changes

Following a topology change, two situations could be considered for the proposed fault location method. First, the shortest path database of the proposed method will be recalculated considering updated information on system current topology. Second, due to different reasons, the current topology of the system may not be updated. Table III shows the result of simulations which have been carried out by switching off lines and simulating faults to address the impact of topology change on the fault location method.

The simulation results illustrate that fault location method would be affected only in certain cases where the switched off line is contributing in shortest path of electromechanical-wave propagation from fault to buses with PMUs. However, the fault location error is acceptable if the switched line is far from the faulty line. As we described in previous subsection, PMUs which are far from faulty line cannot dramatically affect output of the proposed method. Furthermore, to detect a topology change, a pre-defined signal (ping) could be generated at one of the PMU equipped buses and ToAs are measured at other PMU locations. If there is any difference between one of the measured ToAs and corresponding calculated ToAs, a topology change across the shortest path among corresponding two buses is determined.

D. Impact of Availability of PMUs

The other concern associated with wide area measurements based applications is unavailability of PMUs due to various reasons such as communication failure, device failure, etc. In such cases, applications must be robust enough to tolerate unavailability of measurements from one or more PMUs.

Fig. 10 depicts the average error percentage of fault location algorithm versus total number of PMUs assumed to be out of service. After taking each PMU out of service, 20 faults are simulated and average error percentage is used to plot Fig. 10. Similar to previous subsection, three main scenarios were simulated considering three areas in Fig. 9. In Fig. 10(a), faults are simulated in area 1, while dash, dash-dot and dotted lines are related to the cases where out of service PMUs are within areas 1, 2 and 3, respectively. As can be seen, the average error is less than 2% (dash line) even after removing first 6 PMUs from area 1. It can be concluded that even under availability of 5 PMUs in area 1, the method operates with acceptable accuracy. The error remains under 2% even after removing all PMUs in areas 2 and 3, respectively. The same observation could be obtained by looking into Figs. 10(b) and (c). It can be concluded that fault location method on each of the three areas is robust to unavailability of PMUs in other two areas. Since optimal fault location results may be sensitive to placement of PMUs and location of fault occurrence, one can conclude that the proposed method can operate within acceptable error ($< 3\%$) with quite less number of PMUs than what is needed to satisfy the observability requirement suggested by an optimal PMU placement reported in [36].

The last scenario is designed to consider the impact of combination of topology changes and PMU availability on the accuracy of fault location method. Table IV shows the result of fault location method by inserting faults at three different lines while two lines and two PMUs are taken out. In cases 1 and 2, faults occurred on line 1-2 (area 1) while lines (55-59 and 24-70) are taken out but are not contributing to the shortest path to PMUs. In case 1 where the two out of service PMUs (49, 71) are not located in the same area as fault, the fault location error remains the same. In case 2 where the two out of service PMUs (49, 71) are located in the same area as fault, the fault location error slightly increases from 0.32% to 0.41%. In cases 7 and 8, all simulation parameters are the same except switched lines which are selected from those that contribute to the shortest path but located far from the fault point. Similarly, in cases 13 and

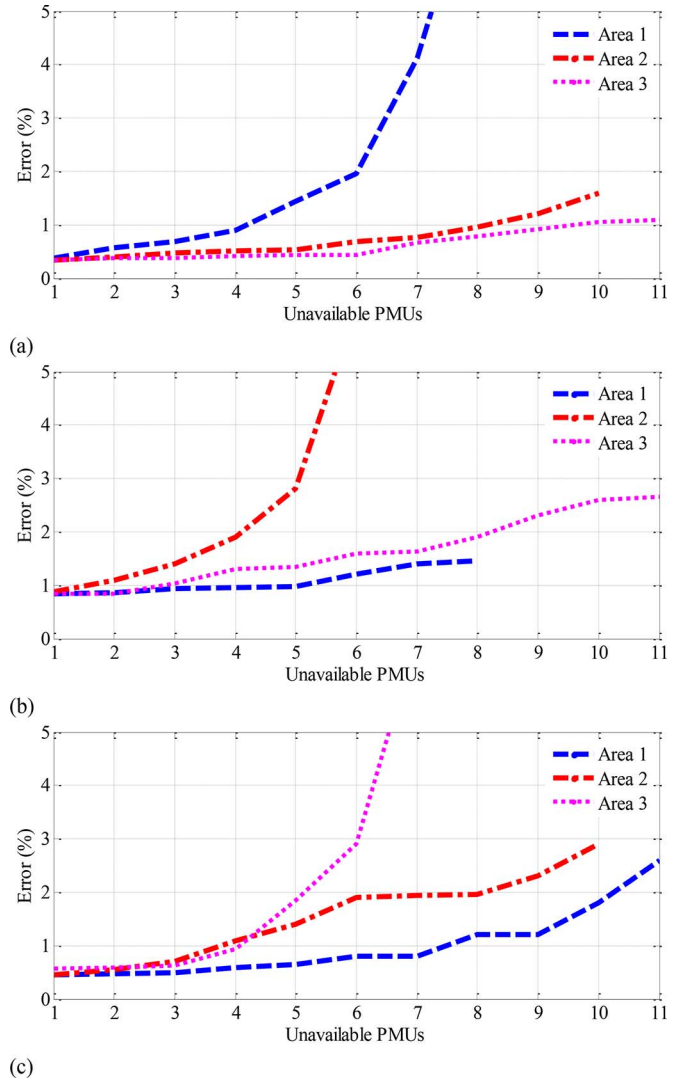


Fig. 10. Effect of unavailability of PMUs on fault location accuracy.

TABLE IV
IMPACT OF COMBINATION OF TOPOLOGY CHANGES AND PMU AVAILABILITY

Case no.	Faulty line	Two Switched lines	Two Unavailable PMUs Location	Error before changes (%)	Error after changes (%)
Switched lines do not contribute in shortest path					
1	1-2	55-59, 24-70	49, 71	0.32	0.32
2	1-2	55-59, 24-70	9, 21	0.32	0.41
3	41-42	3-5, 78-79	1, 110	0.86	0.86
4	41-42	3-5, 78-79	35, 56	0.86	1.07
5	76-118	5-6, 37-39	17, 40	0.49	0.49
6	76-118	5-6, 37-39	71, 94	0.49	0.70
Switched lines contributes in shortest path but located far from fault point					
7	1-2	20-21, 28-29	49, 71	0.32	0.32
8	1-2	20-21, 28-29	9, 21	0.32	0.46
9	41-42	15-17, 69-77	1, 110	0.86	0.86
10	41-42	15-17, 69-77	35, 56	0.86	1.11
11	76-118	22-23, 47-69	17, 40	0.49	0.49
12	76-118	22-23, 47-69	71, 94	0.49	0.71
Switched lines contributes in shortest path and located close to fault point					
13	1-2	5-8, 2-12	49, 71	0.32	0.76
14	1-2	5-8, 2-12	9, 21	0.32	1.48
15	41-42	34-43, 47-49	1, 110	0.86	1.44
16	41-42	34-43, 47-49	35, 56	0.86	2.89
17	76-118	76-77, 94-96	17, 40	0.49	1.63
18	76-118	76-77, 94-96	71, 94	0.49	2.01

14, all simulation parameters are the same except the switched lines are selected from those that contribute to shortest path and are located close to the fault point. From Table IV, it can be concluded that the fault location accuracy would not be affected if PMUs or lines out of service are away from the fault point. The errors would be tolerable even if the out of service PMUs and lines are in the same area where the fault has occurred.

V. CONCLUSION

In this paper a unique fault location methodology based on propagation of electromechanical-wave oscillation in power system is proposed. The main advantages of the proposed methodology over previously established methods are as follows.

- Unlike different wide area measurement based methods which require information from all buses, the proposed method uses measurements from sparsely located PMUs which reduce cost of implementation.
- The calculation burden is less than most of single- or multiple-end fault location methods, since the pre-calculated shortest path database using Dijkstra's algorithm will remain valid until the topology of the power system changes.
- The proposed method could be implemented with PMUs or any other IED devices located in that substation, which can measure and report GPS synchronized phasors.
- The methodology can operate with acceptable accuracy under impacts of topology changes, PMUs bad data or unavailability of one or more PMU measurements, which demonstrate the algorithm is effective even under availability of sparse measurements.

REFERENCES

- [1] Z. Galijasevic and A. Abur, "Fault location using voltage measurements," *IEEE Trans. Power Del.*, vol. 17, no. 2, pp. 441–445, Apr. 2002.
- [2] M. S. Sachdev and M. A. Baribeau, "A new algorithm for digital impedance relays," *IEEE Trans. Power App. Syst.*, vol. PAS-98, no. 6, pp. 2232–2239, Dec. 1979.
- [3] A. A. Girgis, "A new Kalman filtering based digital distance relay," *IEEE Trans. Power App. Syst.*, vol. PAS-101, no. 9, pp. 3471–3480, Sep. 1982.
- [4] T. Kawady and J. Stenzel, "A practical fault location approach for double circuit transmission lines using single end data," *IEEE Trans. Power Del.*, vol. 18, no. 4, pp. 1166–1173, Oct. 2003.
- [5] H. Ha, B. H. Zhang, and Z. L. Lv, "A novel principle of single-ended fault location technique for EHV transmission lines," *IEEE Trans. Power Del.*, vol. 18, no. 4, pp. 1147–1151, Oct. 2003.
- [6] C. E. M. Pereira and L. C. Zanetta, "Fault location in transmission lines using one-terminal post-fault voltage data," *IEEE Trans. Power Del.*, vol. 19, no. 2, pp. 570–575, Apr. 2004.
- [7] Z. Qingchao *et al.*, "Fault location of two-parallel transmission line for non-earth fault using one-terminal data," *IEEE Trans. Power Del.*, vol. 14, no. 3, pp. 863–867, Jul. 1999.
- [8] M. Farshad and J. Sadeh, "Accurate single-phase fault-location method for transmission lines based on k-nearest neighbor algorithm using one-end voltage," *IEEE Trans. Power Del.*, vol. 27, no. 4, pp. 2360–2367, Oct. 2012.
- [9] Y. Liao and S. Elangovan, "Unsynchronized two-terminal transmission-line fault-location without using line parameters," *Proc. Inst. Elect. Eng., Gen. Transm. Distrib.*, vol. 153, no. 6, pp. 639–643, Nov. 2006.
- [10] J. Izykowski *et al.*, "Accurate noniterative fault location algorithm utilizing two-end unsynchronized measurements," *IEEE Trans. Power Del.*, vol. 25, no. 1, pp. 72–80, Jan. 2010.
- [11] E. G. Silveira and C. Pereira, "Transmission line fault location using two-terminal data without time synchronization," *IEEE Trans. Power Del.*, vol. 22, no. 1, pp. 498–499, Feb. 2007.
- [12] M. Davoudi, J. Sadeh, and E. Kamyab, "Parameter-free fault location for transmission lines based on optimization," *IET Gen., Transm. Distrib.*, vol. 9, no. 11, pp. 1061–1068, Aug. 2015.
- [13] M. Davoudi, J. Sadeh, and E. Kamyab, "Time domain fault location on transmission lines using genetic algorithm," in *Proc. 11th Int. Conf. Environment Elect. Eng.*, May 2012, pp. 1087–1092.
- [14] M. Kezunovic and B. Perunicic, "Automated transmission line fault analysis using synchronized sampling at two ends," *IEEE Trans. Power Syst.*, vol. 11, no. 1, pp. 441–447, Feb. 1996.
- [15] A. Gopalakrishnan *et al.*, "Fault location using the distributed parameter transmission line model," *IEEE Trans. Power Del.*, vol. 15, no. 4, pp. 1169–1174, Oct. 2000.
- [16] P. Dutta, A. Esmailian, and M. Kezunovic, "Transmission-line fault analysis using synchronized sampling," *IEEE Trans. Power Del.*, vol. 29, no. 2, pp. 942–950, Apr. 2014.
- [17] J. A. Jiang *et al.*, "An adaptive PMU based fault detection/location technique for transmission lines part I: Theory and algorithms," *IEEE Trans. Power Del.*, vol. 15, no. 2, pp. 486–493, Apr. 2000.
- [18] J. A. Jiang *et al.*, "An adaptive PMU based fault detection/location technique for transmission lines. II. PMU implementation and performance evaluation," *IEEE Trans. Power Del.*, vol. 15, no. 4, pp. 1136–1146, Oct. 2000.
- [19] Y. H. Lin *et al.*, "A new PMU-based fault detection/location technique for transmission lines with consideration of arcing fault discrimination—Part I: Theory and algorithms," *IEEE Trans. Power Del.*, vol. 19, no. 4, pp. 1587–1593, Oct. 2004.
- [20] Y. H. Lin *et al.*, "A new PMU-based fault detection/location technique for transmission lines with consideration of arcing fault discrimination—Part I: Theory and algorithms," *IEEE Trans. Power Del.*, vol. 19, no. 4, pp. 1594–1601, Oct. 2004.
- [21] Y. Liao, "Fault location for single-circuit line based on bus-impedance matrix utilizing voltage measurements," *IEEE Trans. Power Del.*, vol. 23, no. 2, pp. 609–617, Apr. 2008.
- [22] M. Korkali, H. Lev-Ari, and A. Abur, "Traveling-wave-based fault location technique for transmission grids via wide-area synchronized voltage measurements," *IEEE Trans. Power Syst.*, vol. 27, no. 2, pp. 1003–1011, May 2012.
- [23] M. Korkali and A. Abur, "Optimal deployment of wide-area synchronized measurements for fault-location observability," *IEEE Trans. Power Syst.*, vol. 28, no. 1, pp. 482–489, Feb. 2013.
- [24] Y. Chen, D. Liu, and B. Xu, "Wide-area traveling wave fault location system based on IEC61850," *IEEE Trans. Smart Grid*, vol. 4, no. 2, pp. 1207–1215, Jun. 2013.
- [25] S. Azizi *et al.*, "A traveling-wave-based methodology for wide-area fault location in multi-terminal DC systems," *IEEE Trans. Power Del.*, vol. 14, no. 3, pp. 863–867, Jul. 1999.
- [26] J. S. Thorp *et al.*, "Electromechanical wave propagation in large electric power systems," *IEEE Trans. Circuits Syst. I, Fundam. Theory Appl.*, vol. 45, no. 6, pp. 614–622, Jun. 1998.
- [27] A. Semlyen, "Analysis of disturbance propagation in power systems based on a homogeneous dynamic model," *IEEE Trans. Power App. Syst.*, vol. PAS-93, no. 2, pp. 676–684, Mar. 1974.
- [28] P. Dersin and A. Levis, "Feasibility sets for steady-state loads in electric power networks," *IEEE Trans. Power App. Syst.*, vol. PAS-101, no. 1, pp. 60–70, Jan. 1982.
- [29] A. J. Arana, "Analysis of electromechanical phenomena in the power-angle domain," Ph.D. dissertation, Elect. Eng. Dept., Virginia Polytechnic Institute and State University, Blacksburg, VA, USA, Dec. 2009.
- [30] M. Parashar *et al.*, "Continuum modeling of electromechanical dynamics in large-scale power systems," *IEEE Trans. Circuits Syst. I, Reg. Papers*, vol. 51, no. 9, pp. 1848–1858, Sep. 2004.
- [31] E. W. Dijkstra, "A note on two problems in connexion with graphs," *Numer. Math.*, vol. 1, pp. 269–271, 1959.
- [32] D. K. Ranaweera, "Comparison of neural network models for fault diagnosis of power systems," *Elect. Power Syst. Res.*, vol. 29, pp. 99–104, 1994.
- [33] A. Abdullah *et al.*, "Test bed for cascading failure scenarios evaluation," presented at the IPST 2013, Vancouver, BC, Canada, Jul. 2013.
- [34] N. Abramson, *Information Theory and Coding*. New York, USA: McGraw-Hill, 1983.

- [35] R. Christie, Power system test archive, Aug. 1999. [Online]. Available: <http://www.ee.washington.edu/research/psca>
- [36] S. Azizi, A. Dobakhshari, A. N. Sarmadi, and A. M. Ranjbar, "Optimal PMU placement by an equivalent linear formulation for exhaustive search," *IEEE Trans. Smart Grid*, vol. 3, no. 1, pp. 174–182, Mar. 2012.



Ahad Esmailian (S'08) was born in Iran in 1987. He received the B.Sc. and M.Sc. degrees in power system engineering from the University of Tehran, Tehran, Iran, in 2009 and 2012, respectively.

Currently, he is a Graduate Student with Texas A&M University, College Station, TX, USA. His main research interests are power system protection, fault location, and application of intelligent methods to power system monitoring and protection.



M. Kezunovic (S'77–M'80–SM'85–F'99) received the Dipl. Ing. degree in electrical engineering from the University of Sarajevo, Sarajevo, Bosnia and Herzegovina, in 1974 and the M.S. and Ph.D. degrees in electrical engineering from the University of Kansas, Lawrence, KS, USA, in 1977 and 1980, respectively.

He is the Eugene E. Webb Professor and Site Director of Power Engineering Research Center (PSerc), an NSF I/UCRC at Texas A&M University, College Station, TX, USA. He is also the Director of the Smart Grid Center. He has published more than 450 papers, given over 100 seminars, invited lectures and short courses, and consulted for over 50 companies worldwide. He is the Principal of XpertPower Associates, TX, USA, a consulting firm specializing in automated fault analysis and intelligent electronic device testing. His main research interests are digital simulators and simulation methods for relay testing, as well as the application of intelligent methods to power system monitoring, control, and protection.

Dr. Kezunovic is a Fellow of CIGRE and a Registered Professional Engineer in Texas.